SIMULATION BASED MODELING OF THE ELASTIC PROPERTIES OF STRUCTURAL COMPOSITE LUMBER

Laszlo Bejo

Senior Research Scientist
University of Western Hungary
H-9400 Sopron, Ady E. u. 5.
Hungary
Formerly,
Graduate Research Assistant
WVU, Division of Forestry

and

Elemer M. Lang†

Associate Professor
West Virginia University
Division of Forestry
Morgantown, WV 26506-6125

(Received September 2003)

ABSTRACT

Structural composite lumber (SCL) products were introduced into the construction practice several decades ago. Their apparent advantages over traditional lumber did not generate copious research interests. However, increasing demands for structural materials coupled with the decreasing quality and quantity of raw materials are forcing the industry to introduce short rotation trees or species having unfavorable properties into the manufacturing processes. Consequently, there is a need for research to further enhance the effective use of renewable natural resources.

This article describes the development of simulation models that estimate the bending and orthotropic compression modulus of elasticity (MOE) of laminated veneer lumber (LVL) and parallel strand lumber (PSL). The Monte Carlo simulation-based routines use the physical/mechanical properties of primary constituting elements, obtained from probability distributions, to calculate a particular property of the composite system. Furthermore, the orthotropic behavior of the wood constituents due to their position in the composite is modeled by well-established theoretical/empirical equations. Results and experimental validation regarding the geometric, physical, and mechanical attributes showed reasonably good agreement between simulated and experimental values. Developed models have good potential for predicting the elastic parameters of composites using new raw materials or novel design features.

Keywords: Wood composites, elastic properties, simulation modeling.

INTRODUCTION

Traditionally, solid wood is the raw material most frequently used for residential construction in the United States. Environmental concerns and the declining quality and quantity of timber resources have driven the industry toward alternative solutions. Such pressures triggered the development of structural wood-based composite materials. These are excellent substitutes for solid wood in many aspects: they are lightweight, strong, and durable. Moreover, some of the species/products combinations exhibit higher and more consistent mechanical properties due to the densification during the consolidation process; and they demonstrate better dimensional stability than those of solid wood. Many of their properties can also be engineered to a certain extent.

† Member of SWST.

Manufacturers of wood-based structural composites are constantly seeking to improve the mechanical properties of their products. The traditional trial-and-error approach is costly, time-consuming, and often not feasible. A better alternative is using simulation modeling to optimize the various manufacturing parameters (Law and Kelton 1991). Using a reliable probability-based simulation model, one can demonstrate the effects of changing properties or relative position of the constituting materials on the final performance of the products without having to run actual manufacturing trials.

A long-term research explored the orthotropic mechanical properties of five hardwood species (Lang et al. 2000, 2002, 2003) at WVU, Division of Forestry and University of Western Hungary. Species included: red oak (*Quercus rubra*), turkey oak (*Quercus cerris*), quaking aspen (*Populus tremuloides*), true poplar (*Populus x. Euroamericana cv. Pannonia*), and yellow-poplar (*Liriodendron tulipifera*) as potential raw materials for structural composite manufacture.

As the concluding part of the comprehensive project, the objectives of this study were to develop and validate probability-based simulation models that can describe the bending and orthotropic compression MOE of parallel strand lumber (PSL) and laminated veneer lumber (LVL), based on the geometry and orthotropic elastic parameters of their constituents. The stochastic parameters of three North American species were incorporated into simulation models. Such simulation routines may provide an inexpensive tool for evaluating the effect of novel raw materials or other modifications on the expected performance of these structural composite products. Moreover, the models were validated by comparing their predictions to properties measured on commercial LVL and PSL produced from yellow-poplar structural veneers.

LITERATURE REVIEW

Modeling physical and mechanical properties requires a thorough understanding of spatial structure of the composites. An early simulation model described the structure of paper as consisting of several layers of fibers and interfibrillar spaces or pores (Kallmes and Corte 1960; Kallmes et al. 1961). This work provided a basis for developing a mathematical model that depicts randomly packed, short-fiber-type wood composites (Steiner and Dai 1993; Dai and Steiner 1994a, b.) Results of this investigation were used in a Monte Carlo simulation program that can model different types of mats, and analyze them for various important geometric characteristics (Lu et al. 1998). The program can also determine the effect of sampling zone size on the measured density distribution. Harris and Johnson (1982) dealt with the characterization of flake orientation in flakeboards. They pointed out that unbounded distributions are not appropriate for this purpose and suggested a bounded distribution to provide angles between 0 and π radians.

Some researchers attempted to provide a detailed explanation and to simulate certain aspects of particle mat behavior during consolidation. Suchsland (1967) summarized the mat formation, heat- and moisture movement and stress-behavior of particleboard mats. He provided an explanation for the formation of horizontal and vertical density distributions, and showed how pressing parameters influence the latter. Humprey and Bolton (1989) made an in-depth analysis of the multidimensional unsteady-state heat and moisture transfer during hot pressing. They built a model based on a modified finite difference approach that could predict temperature, moisture content, vapor pressure, and relative humidity in different layers of a mat.

Several works dealt with the compression behavior of strand mats throughout the pressure cycle. Dai and Steiner (1993) developed a theoretical model to describe the compression response of randomly formed wood flake mats. Their predictions agreed with experimental results reasonably well. Two further models, using somewhat different approaches to reconstruct the OSB mat structure and to predict the stress-strain relationship during consolidation, provided improved estimation of stress development (Lang and Wolcott 1996a,b; Lenth and Kamke 1996a,b.) It has been proposed that a combination of these two models characterizes the entire stress-strain curve somewhat better than the earlier approaches.

Physical and mechanical properties of wood-based composites are closely related to density. Vertical and horizontal density distribution (VDD and HDD) generated much research interest. Suchsland and Xu (1989, 1991) developed physical models to examine the effect of HDD on thickness swelling and internal bond strength. They concluded that the durability of flakeboard is substantially affected by the severity of the horizontal density distribution. Xu and Steiner (1995) presented a mathematical concept for quantifying the HDD. Another study (Wang and Lam 1998) linked a simulation program with an experimental mat through a robot system that deposited flakes in the simulated positions. Predicted and actual HDD showed good agreement.

Harless et al. (1987) created a very comprehensive simulation model that can regenerate the VDD of particleboard as a function of the manufacturing process. Other research in this area included the characterization of VDD using a trigonometric density function (Xu and Winistorfer 1996), and a simplified physical model to examine how the number of flakes, face flake moisture content, and press closing time affect VDD (Song and Ellis 1997).

Zombori (2001) formed a series of linked simulation and finite element models that could, in turn, recreate the geometric structure, compression behavior, and heat and mass transfer of oriented strand board. These models could predict the inelastic stress-strain response, environmental conditions, moisture content, and density at different points within the panel. His results—some of which are applicable to other composites, like particleboard, too—were in reasonable qualitative agreement with laboratory test data.

Xu and Suchsland created most of the models simulating physical and mechanical properties of wood composites. They dealt with the linear expansion of particleboard (1997), followed up by a study discussing the effect of out-of-plane orientation (1998a). In these works, they made use of the off-axis MOE, determined by the Hankinson's formula. Results of these studies helped to develop another model (Xu and Suchsland 1998b) to simulate the uniaxial MOE of composites with uniform VDD, based on the total volumetric work. Xu (1999) modified this simulation to investigate the effect of VDD on the bending MOE of composites, using the summation of stiffness values of discrete layers. This model was applied to evaluate the effect of percent alignment and shelling ratio on the MOE of OSB (Xu 2000). Simulation results agreed well with experimental and literature data.

Triche and Hunt (1993) modeled parallel-aligned wood strand composites using finite element analysis. They created small scale, parallel-aligned strand composites that can be considered as physical models for LVL or PSL. The applied model accounted for the effect of densification, adhesive penetration, and crush-lap joints, and estimated the tensile strength and MOE of the specimens with excellent accuracy. In a recent study, Barnes (2001) modeled the strength properties of oriented strand products. He introduced the concept of stress transfer angle to assess the effect of strand length and thickness on the mechanical properties of composites. He found good agreement between experimental and model-predicted MOE, MOR, and tensile strength values.

Wood-based composite lumbers, such as LSL, LVL, or PSL, are relatively new products that generated less research interest than did composite panels. Results of research works on composite panels can be applied to these products with care. Meanwhile, available literature does not seem to contain simulation studies that are directed specifically towards modeling the geometric structure and mechanical properties of these structural composites.

THEORETICAL BACKGROUND

Although the structure of the two composite types involved in this study is largely different, the fundamental principles used in the simulation of their elastic properties are the same. The effective bending modulus of composites is defined by the stiffness summation of discrete layers (Bodig and Jayne 1982) as follows:

$$E = \frac{\sum E_i I_i}{I} \tag{1}$$

where: E, I – composite MOE and 2nd order moment of inertia of the cross-section, respectively;
E_i, I_i – layer MOE and moment of inertia of the i^{th} layer with respect to the composite's neutral axis, respectively.

This theory assumes equal compression and tension stiffness and pertains directly to layered composites like glued-laminated beams, LVL, and plywood. However, it can be applied to nonlayered systems, such as PSL, as well. In this case, the above summation involves individual strands, rather than layers. The compression and tension modulus of elasticity may be different for some wood species depending on the moisture content as reported by Conners and Medvecz 1992. Therefore, the MOE of a constituent depends on whether it is located in the compression or the tension zone. Some elements are subjected to both compression and tension stresses, and the orthotropic response of woody materials depends on their orientation relative to the principal material coordinates of the composite. Furthermore, the inherent densification and resin penetration may significantly alter the modulus of elasticity, thus impairing the computed results. These points are important to consider during any model development.

The determination of compression MOE is based on the calculation of the external work applied to a body and the internal energy stored therein. These quantities are equal in the linear elastic region. Xu and Suchsland (1998b) derived the following equation from this equality:

$$E = \frac{\sum E_i V_i}{V} \qquad (2)$$

where: E, V – compression MOE and total volume of the composite;
E_i, V_i – compression MOE and volume of the i^{th} constituent.

The above-discussed simple theories govern the behavior of SCL materials in many loading applications. However, the stochastic nature of spatial arrangement of the constituents, the natural variability of wood properties, and the unpredictable effects of manufacturing processes represent real challenges in forecasting mechanical properties of the final products. Without pursuing absolute precision, our goal was to reasonably model the elastic behavior of LVL and PSL on the basis of the properties of their constituents.

MODEL DEVELOPMENT

In general, models developed during this study include three major modules that provide electronically stored information for validation and further computations. First the spatial geometric structure of the composite in question is characterized using empirical probability distributions and/or deterministic variables. In the second step, an appropriate routine allocates stochastic MOE values to each constituent in the principal anatomical directions as input variables for the orthotropic models. The computed direction-defined stiffness quantities are then modified by randomly assigned densification values. Finally, the modulus of elasticity in bending or in compression can be calculated using Eqs. (1) or (2).

Although the mechanical and physical properties of structural composites are more consistent than those of solid wood, still a vast array of interacting variables governs their properties and behavior under load. To maintain the mathematical tractability of the models, several simplifying assumptions had to be made. The major hypothesis of this research was that a single cross-section might represent the entire beam or column reasonably well. This assumption allowed the reduction of the three-dimensional problem to a much simpler in-plane modeling. Further simplifications used in the models included the following:

- Composites are treated as prismatic beams; i.e., their cross-section does not change along the length; and the constituents are represented by their individual, true size sections corresponding to their relative orientation.
- Veneers used for layers and strands are peeled perfectly tangential to the annual ring (i.e., their plane is LT).
- A continuous glueline provides perfect adhesion between the layers or strands.

- The applied glue does not alter the MOE of the layers or strands significantly.
- The grain orientation of an LVL layer is always parallel with the longitudinal axis of the beam; the grain orientation of a PSL strand is always parallel with the longitudinal axis of the strand.
- The layup is random; the MOE values of the layers or strands are independent of their position. In practice for LVL, the stress wave sorting for face and core designation is visually overridden because of defects. Thus, this assumption may be justified.
- The thickness of a layer in LVL is constant. Irregularities, such as crushed-lap joints that connect two veneer sheets and the inherent voids have counteracting effects on strength and stiffness, and are disregarded.
- PSL strand cross-sections are rectangular in shape; strands are not bent or distorted.
- PSL strand width is constant (25 mm).
- The densification of a PSL strand is independent from its position within the billet.
- The neutral plane in bending coincides with the symmetry axis of the cross-section.

SIMULATING THE GEOMETRY OF COMPOSITES

Figure 1 shows the geometric features of LVL and PSL. The composites are placed in an orthogonal coordinate system, where x is the longitudinal axis of the beams, y is the main cross-sectional orientation of the constituents, and z is perpendicular to both x and y. One can easily realize that x, y, and z are correspondingly equivalent to the *L, T,* and *R* principal anatomical directions in solid wood. Using these axes, it is possible to define *load orientation* (θ) and *strand/layer orientation* (ϕ) relative to normal stresses acting in the beam. These angles are analogous to grain and ring angle in solid wood, respectively.

For LVL, the simulation of the geometric properties included the following steps:

- Establishing the number of layers. This is a deterministic variable that depends on the particular material being simulated. In the present case, the number of layers was 15.
- Assigning original and final thickness values to each layer from their respective probability distributions. The two outer layers (face) at each side and the rest (core) were treated differently because of the different densification during the pressing process.
- Calculating cross-section (A_i), 2nd order moment of inertia around the symmetry axis of the composite (I_i), and volume fraction (V_i) for each layer.

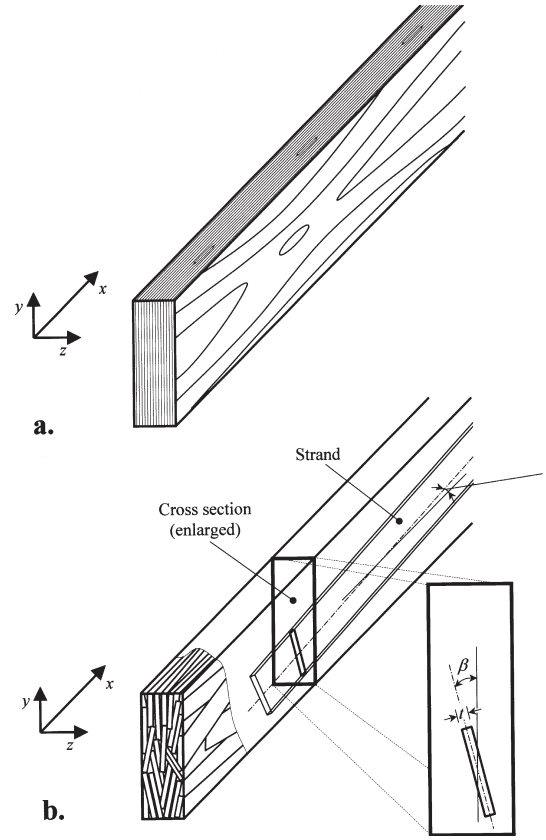

FIG. 1. The geometric structure of LVL (**a**) and PSL (**b**).

Figure 2a shows the comparison of actual and simulated cross-sections for LVL. The stochastic parameters of the spatial structure are the thickness of the layers and their locations within the cross-section.

To electronically recreate the spatial structure of PSL, we developed an inverse, iterative simulation routine. The method is inverse, because it generates the projected-densified thickness of strands first. It randomly assigns original thickness values in the second step; then it computes the projected width and projected cross-sectional

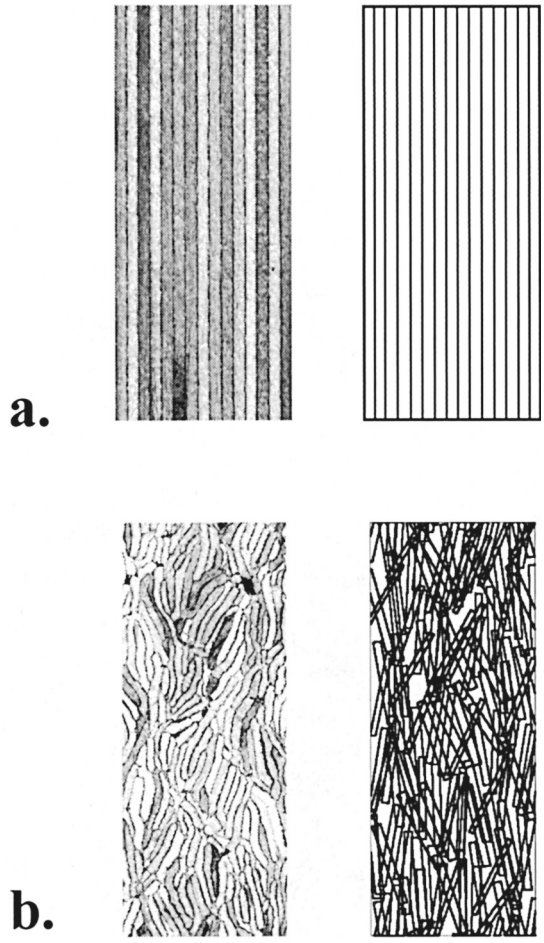

FIG. 2. Actual and simulated cross-sections of LVL (**a**) and PSL (**b**).

area according to the orientation and preserves the densification of the strands. The process is repeated until a pre-established area coverage criterion is satisfied. Note that the densification, affecting the MOE of the strand, is defined by the original and non-projected densified thickness.

Steps of the simulation process included the following:

- Choosing the y and z cross-sectional dimensions.
- Simulating the number of strands. In PSL, the number of constituents is a random variable, established by generating the number of strands per in^2 (u), and multiplying this number by the cross-sectional area of the beam.
- Assigning projected-densified and original strand thickness (t and t_o), longitudinal *strand angle* (α), and a cross-sectional *strand deviation* (β) values to each strand. The model neglects the deviation of the strands' longitudinal axis from the x-y plane. The original width of the strands is 25 mm, except for one strand, which has a smaller width. This strand reflects the fractional part of the strand number (u).
- Calculating densifications from t and t_0;
- Summation of projected-densified strand areas and checking the area coverage criterion;
- Arranging strands in both the y and the z directions. To achieve an even coverage, strand centroids are distributed uniformly in a systematic way, rather than randomly.
- Calculating A_i, V_i and I_i (flatwise and edgewise), for each constituent. Strands that protrude beyond the boundary of the beam cross-section are handled according to the torus convention (Hall 1988).

The strand deposition process results in overlapping strand areas and holes as demonstrated on Figure 2b. These overlapping areas and holes represent distorted strands that fill the sectional area of PSL in reality. Note, that the horizontal dislocation of strands has no effect on the stiffness of the composite or a particular individual strand in bending. In case of compression, the location of a strand within the cross-section is indifferent regarding the composite MOE. In the simulated cross-section, a projected area, two angles, and the position of the strand's centroid represent each constituent.

Stochastic parameters, mentioned above, were generated using probability density functions fitted to experimental databases. Table 1 summarizes the type and parameters of each function. Figure 3 shows two sample histograms, created from experimental data. The diagrams include the overlaid probability density functions, along with a histogram of 1000 simulated random deviates. Visual appraisal and standard statistical tests (Kilmogorov-Smirnov; χ^2) helped to identify the best fitting probability density functions.

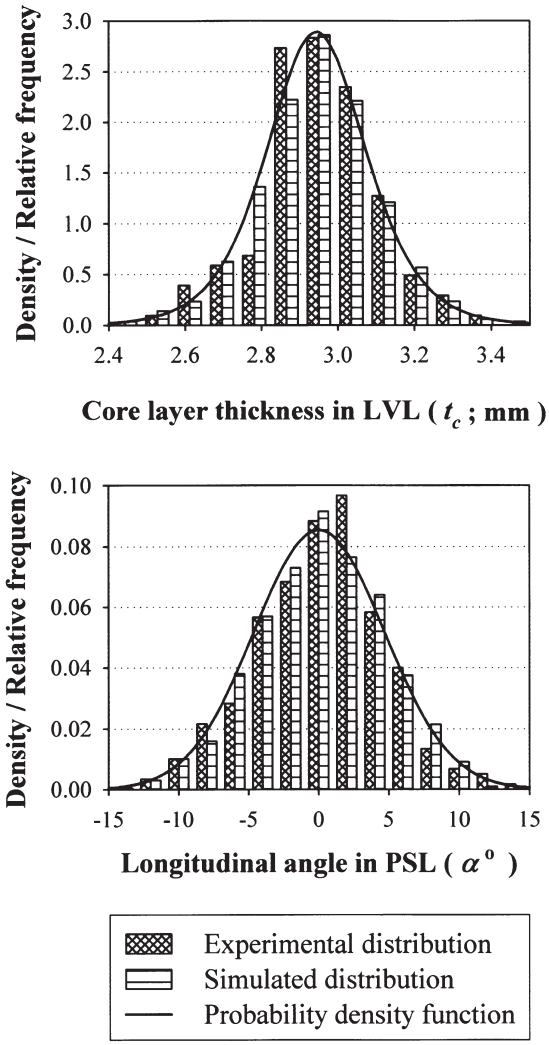

FIG. 3. Sample histograms of the geometric input parameters with the probability density functions overlaid.

MODELING THE ELASTIC PARAMETERS OF THE CONSTITUENTS

The MOEs of the constituents were generated in a three-step process:

1. Determining the orientation of the constituents relative to the direction of stresses.
2. Assigning compression and/or tension MOE values to the constituents in the given orientation. This involves the use of orthotropic theories, which require MOE values in various anatomical directions, as input parameters. Experimental determination of these parameters and the validation of the orthotropic models have been presented in two former articles. The model simulates compression and tension MOE using the three-dimensional Hankinson's formula (Lang et al. 2002) and a combination of the Hankinson's formula and the orthotropic tensor theory (Lang et al. 2003), respectively. The elastic input parameters for these formulas are generated assuming normal distribution.
3. Modifying the constituents' MOE values to account for the effect of densification. The model increases the MOE denomination of the veneers or strands, due to density increase during hot pressing, based on experimental, second-order densification curves.

We developed the simulation routines using the FORTRAN 90 programming environment. The source code includes four programs, as well as several different functions to generate random data from different distributions, so as to simulate the orthotropic tensile and compression MOE along with the densification effect. A sample flowchart is included in Figure 4, demonstrating the simulation process for PSL.

A module stores the species-specific input parameters for quaking aspen (*Populus tremuloides*), red oak (*Quercus rubra*), and yellow-poplar (*Liriodendron tulipifera*). These parameters include the summary statistics and probability density functions of input E values, density, and sectional dimensions. The routine can be easily extended to cope with new species by adding their parameters to this module.

EXPERIMENTAL VALIDATION

Materials and Methods

Materials used for validation of the models were commercial LVL and PSL. While the LVL had only yellow-poplar veneers, PSL contained approximately 25% southern yellow pine (*Pinus* spp.) strands. Note that the input elastic properties in the principal material directions are generated randomly from probability density

TABLE 1. *Type and parameters of the probability density functions of the stochastic input variables.*

Input parameter	Unit	Probability density function	Function parameters [a]		
			μ	σ	α
		Original veneer thickness			
Quaking aspen	mm	Extreme Value A	3.108	0.069	—
Red oak	mm	Logistic	3.046	0.048	
Yellow-poplar	mm	2-param. Weibull	—	3.162	42.761
		LVL [b]			
t_o	mm	Normal	2.760	0.140	—
t_c	mm	Logistic	2.940	0.090	—
		PSL			
u	#/in^2	Normal	11.64	0.36	—
t	mm	Normal	2.051	0.391	—
α	°	Normal	0.030	4.668	—
β	°	Normal	2.991	14.709	—

[a] μ – location; σ – scale; α – shape.
[b] t_o – thickness of the two outside layers on both sides ; t_c – thickness of the remaining (core) layers.

functions. The obvious overlap of the probability density functions of MOE for the two species may introduce only a few outliers into the model. Consequently, the effect of mixture of species was neglected. All testing materials were kept in a temporary environmental chamber at approximately 21ºC temperature and 65% relative humidity (RH) during the entire duration of the project. Moisture contents of the test materials were periodically checked on control specimens using standard ASTM procedure (ASTM 1996c).

In the first phase of the validation, twenty simulated cross sections for both LVL and PSL were compared to actual sections of the materials. The links between the actual and simulated sections were the number of layers and the number of strands per in^2 (u) for LVL and PSL, respectively. Assigning unit length to the generated cross-sections, the density of the simulated composites could be calculated and compared to actual values. Experimental densities were measured and calculated using structural size composites. Additionally, for LVL the total simulated thickness of the beam was compared to actual thickness; and, for PSL the cumulative, projected strand areas (ΣA_i) and the cumulative moment of inertia (ΣI_i) of the strands were measured up to target quantities.

Twenty structural size beams of LVL and PSL, tested both edgewise and flatwise using a 4-point bending setup over 2.44-m span, provided experimental bending MOE data. The nominal cross-sections were 45 mm × 95 mm and 75 mm × 140 mm for LVL and PSL, respectively. The procedure strictly followed the specification of the relevant ASTM standard (ASTM 1996a). The Baldwin type testing apparatus had a load cell with 180 kN capacity. A linear potentiometer having ± 0.01-mm accuracy measured the relative deflection of the shear free section of the beam. Load-deflection data were collected in real time using a computerized acquisition system.

Compression MOE determination followed the specification of ASTM standard D 143–94, secondary method. Accordingly, specimen dimensions were: 25 × 25 × 100 mm. For evaluation of the orthotropic nature of the composites, the principal dimensions of the specimens were rotated systematically by 45º increments, which resulted in six groups of load and strand orientation (ϕ' and θ'). Note that ϕ' and θ' are analogous to grain and ring angle of solid wood specimens. When a particular combination of load/strand orientation was required, LVL sections were glued side-to-side to provide 100 mm of specimen length. Ten replications of each combination provided statistically reliable experimental compression MOE data. Compression load application and the double-sided strain measurements were conducted on an MTS

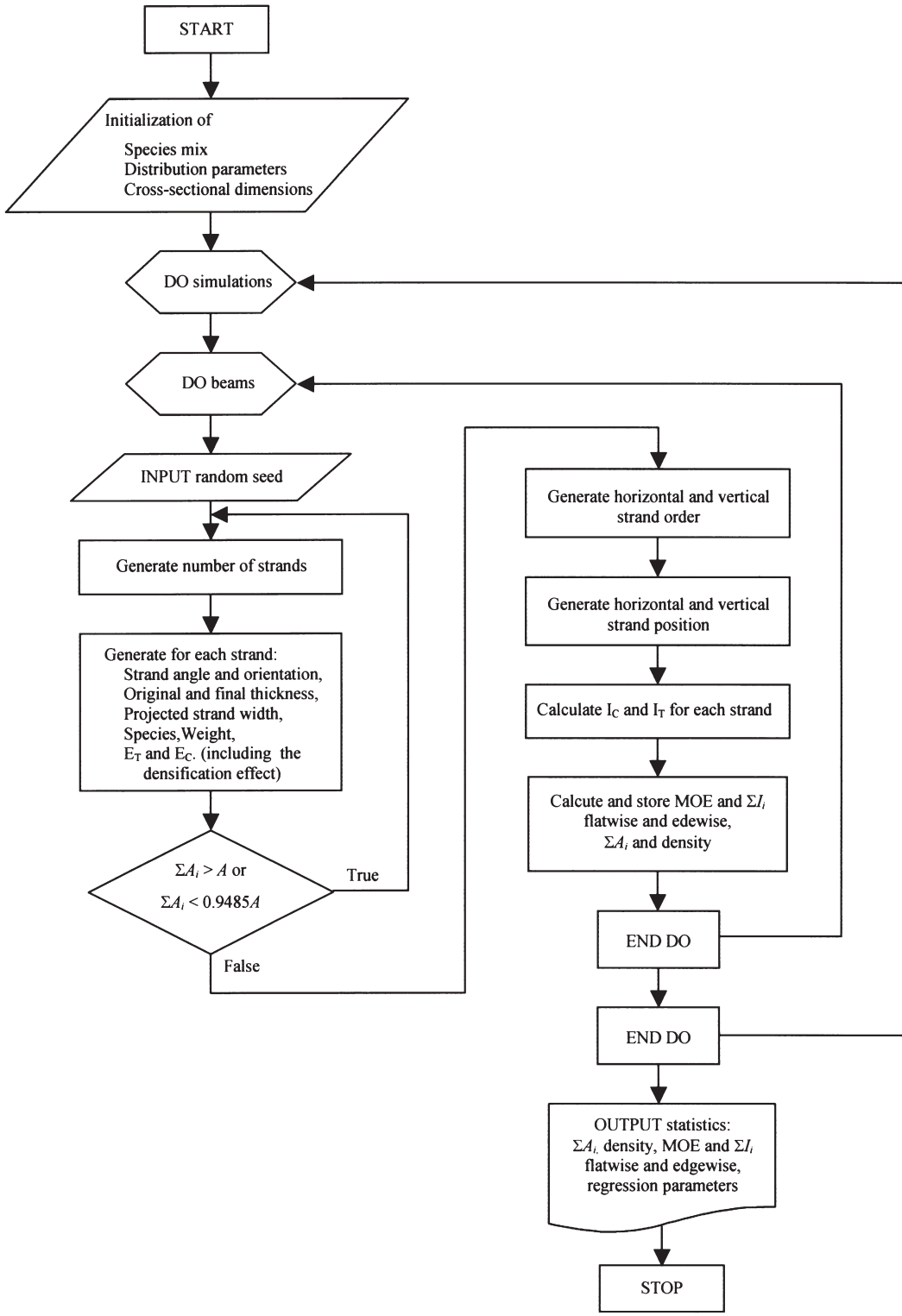

FIG. 4. Flowchart of the bending MOE simulation of PSL.

servo-hydraulic universal testing machine, equipped with a 10 kN ±1N load cell. Pairs of strain data were obtained continuously using two MTS clip-on gauges. The interested reader can find a detailed description of the specimen preparation practice and experimental technique in a related publication (Lang et al. 2002). Both for bending and compression, the collected load-deformation data were within the linear elastic region.

Bending MOE simulation consisted of generating twenty LVL and PSL beams, and calculating their MOE both in flatwise and edgewise orientations. The cross-sectional dimensions of the simulated beams were the same as the nominal dimensions of the tested specimens. The entire Monte Carlo simulation was repeated twenty times resulting in 400 cross-sections where each represented a particular composite beam edge- or flatwise.

Compression model validation was similar to the above procedure, but it involved 20 replications of only 10 simulated specimens in each of six orientations per composite types. This process resulted in a total of 2400 simulation runs.

Standard statistical procedures including t-test, Mann-Whitney Rank Sum Tests helped to evaluate the differences between experimental and simulated results. All tests were conducted at 95 % confidence level ($\alpha = 0.05$).

RESULTS AND DISCUSSION

To confirm the validity of the first module, the simulated physical properties, including density and geometrical characteristics, were compared to experimental data. Table 2 contains the summary statistics of the results. Simulated quantities are average values of the mean, standard deviation, minimum, maximum, and skewness calculated from the twenty Monte Carlo simulations, containing twenty beams for each composite type.

For LVL, good agreement between actual and predicted thickness values could be detected. It means that the selected probability density functions described the variations in face and core veneer thickness reasonably well. In contrast, the model significantly underestimated the density when the simulated values were compared to actual densities measured on 2.44-m-long LVL beams. Our initial hypothesis was that the overlapping veneer joints and the coupling through-the-width voids have no effect on the mechanical properties of LVL. Apparently, this is not true regarding density because the volume of dense LVL containing an extra layer is significantly bigger than that of void volume in the beam. However, the comparison of model predicted

TABLE 2. *Simulated and experimental geometric and physical properties of LVL and PSL.*

Property	Unit	Source	Mean	STD[1]	Min.	Max.	Skewness
			LVL				
Thickness	mm	Sim.	43.0	0.50	42.1	43.9	0.005
		Exp.	43.6	0.15	43.1	44.0	0.013
Density	kg/m^3	Sim.	511.0	10.00	492.0	530.0	–0.100
		Exp.	566.0	11.00	541.0	584.0	0.078
		Exp.[2]	509.6	9.90	498.6	529.7	0.097
			PSL				
ΣA_i	cm^2	Sim.	103.7	1.4	101.4	106.1	0.029
$A_{composite}$	cm^2	Target	106.5	——-	——-	——-	——-
ΣI_i	cm^4	Sim.	498.3	6.8	486.9	509.7	0.001
$I_{composite}$	cm^4	Target	515.1	——-	——-	——-	——-
Density	kg/m^3	Sim.	673.0	11.0	652.0	694.0	–0.037
		Exp.	673.0	16.0	640.0	708.0	–0.122

Sample size: n = 20,
1 – Standard Deviation,
2 – Density of overlapping veneer-joint free LVL.

densities to measured ones on joint-free LVL sections demonstrated excellent agreement.

As it was expected, the model slightly underpredicted the simulated cross-sectional area of PSL strands (ΣA_i) because of the built-in area coverage constraint. In reality, PSL contains longitudinal voids due to the imperfect packing of strands. See Fig. 2b where the black areas represent through-the-length holes of a 10-mm-long PSL section. These voids have technological advantage in releasing internal steam pressure from the billet after high-frequency die consolidation. The approximately 97.4% average area coverage that resulted from the simulation is a good approximation of a real PSL cross-section. Due to the area coverage criterion, the model underpredicted the 2nd order area moment of inertia of the beam (ΣI_i) by approximately 5% on average basis. The target or actual cross-sections contain voids that cannot be handled during the experimental determination of bending MOE. This is an inherent bias of the testing procedure that we have accepted. Conversely, the simulated density, which showed excellent agreement with actual values, encouraged the acceptance of this simulation routine.

Table 3 contains the summary statistics of simulated and experimental bending MOE of LVL and PSL. Note that the data of simulation results are the average of twenty batches of twenty runs, and not the standard deviation of averages but the average of standard deviations are listed. We do believe that this method provided better estimation of expected minimum and maximum values. Figure 5 provides a quick visual overview of the results. The simulated bending MOE values of LVL in both directions were slightly lower compared to observed data. The differences, however, were not significant, especially in flatwise application and resulted mainly from the higher standard deviation of test results. It does appear that the effect of overlapping veneer joints (their presence/absence and location) manifested in higher variability.

The model significantly and consistently overestimated the bending MOE of PSL beams. There are several plausible explanations for this phenomenon related to the manufacturing tech-

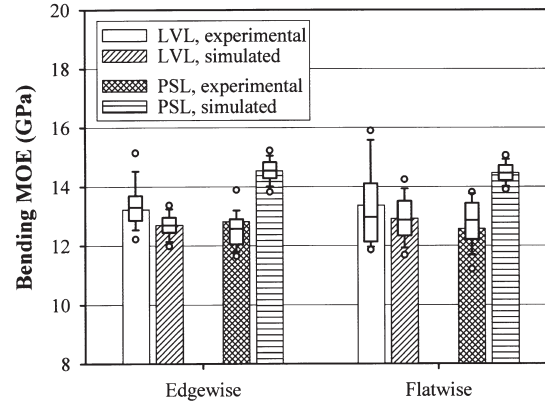

FIG. 5. Experimental and simulated bending MOE of LVL and PSL.

TABLE 3. *Comparison of simulated and experimental bending MOE of LVL and PSL.*

Direction of Bending	Source	n[1]	Mean (GPa)	STD[2] (GPa)	Min. (GPa)	Max. (GPa)	Skewness
			LVL				
Flatwise	Sim.	20×20	12.91	0.79	11.40	14.64	0.100
	Exp.	20	13.36	0.72	12.20	15.16	0.212
Edgewise	Sim.	20×20	12.70	0.41	11.95	13.49	0.063
	Exp.	20	13.22	1.21	11.85	15.90	0.022
			PSL				
Flatwise	Sim.	20×20	14.46	0.34	13.83	15.10	0.041
	Exp.	20	12.57	0.57	11.64	13.92	–0.087
Edgewise	Sim.	20×20	14.54	0.40	13.78	15.29	–0.052
	Exp.	20	12.82	0.75	11.18	13.81	0.115

[1] Replications/sample size.
[2] Standard deviation.

nology of the product. However, based on the results of the compression MOE simulation and experimental data, we believe that the inaccuracy of the orthotropic model to estimate the MOE of composites, and neglecting the out of *x-y* plane deviation of strands are the major reasons for these overestimations. Currently the model is under expansion by introducing an additional random variable: γ, defined as the deviation angle from the *x-y* plane. Some improvement in accuracy is expected, though the effect of rolling shear deformation in an off-axis strand still will not be encountered.

The compression MOE simulation routine was run 2400 times to provide an adequate predicted database. Table 4 contains the average statistical parameters of the twenty compression MOE simulations in the six selected combinations of orientation, along with the experimental statistics per product type. Figure 6 offers a quick comparison between observed and simulated results in each direction for LVL and PSL.

Excellent fit of predictions to observed values was identified for both LVL and PSL at 0º/-; 45º/0º; 90º/0º ϕ′/θ′ angle combinations. This indicated that the orthotropic models described the changes of MOE in the *x-y* plane exceptionally well; and the inherent shear deformations—mostly in the LT anatomical plane of the constituents—had no explicit effect on the elastic performance of the products.

Once the direction of normal stresses deviated from the principal *x-y* plane of the composites, the model consistently and significantly overestimated the modulus of elasticity. This fact indicated that neither the 3D Hankinson's formula nor the 3D orthotropic tensor approach could model the true elastic response of three dimen-

TABLE 4. *Comparison of simulated and experimental compression MOE of LVL and PSL at different load (φ′) and strand (θ′) orientations.*

φ′	θ′	Source	Mean (GPa)	STD[1] (GPa)	Min. (GPa)	Max. GPa)	Skewness
			LVL				
0°	***—***	***Sim.***	***11.33***	***0.46***	***10.61***	***12.11***	***0.065***
		Exp.	***11.87***	***1.06***	***9.71***	***13.34***	***0.142***
45°	***0°***	***Sim.***	***0.79***	***0.02***	***0.75***	***0.83***	***0.109***
		Exp.	***0.87***	***0.07***	***0.76***	***1.01***	***0.004***
45°	90°	Sim.	1.52	0.06	1.43	1.61	0.124
		Exp.	0.84	0.06	0.75	0.96	0.545
90°	***0°***	***Sim.***	***0.41***	***0.01***	***0.39***	***0.43***	***0.108***
		Exp.	***0.44***	***0.03***	***0.41***	***0.44***	***–0.022***
90°	45°	Sim.	0.49	0.02	0.47	0.51	0.170
		Exp.	0.29	0.05	0.23	0.35	0.112
90°	90°	Sim.	0.82	0.03	0.77	0.87	0.146
		Exp.	0.37	0.03	0.31	0.42	0.135
			PSL				
0°	***—***	***Sim.***	***13.34***	***0.43***	***12.63***	***13.99***	***–0.139***
		Exp.	***13.20***	***2.09***	***10.71***	***17.28***	***0.128***
45°	***0°***	***Sim.***	***1.06***	***0.04***	***1.00***	***1.11***	***–0.081***
		Exp.	1.08	0.11	0.86	1.25	–0.002
45°	90°	Sim.	1.90	0.06	1.80	1.99	–0.035
		Exp.	0.64	0.05	0.55	0.73	–0.100
90°	***0°***	***Sim.***	***0.51***	***0.01***	***0.52***	***0.56***	***–0.141***
		Exp.	***0.48***	***0.07***	***0.39***	***0.60***	***–0.221***
90°	45°	Sim.	0.64	0.02	0.61	0.67	–0.035
		Exp.	0.30	0.03	0.25	0.36	0.186
90°	90°	Sim.	1.02	0.04	0.97	1.08	–0.053
		Exp.	0.23	0.03	0.19	0.28	–0.254

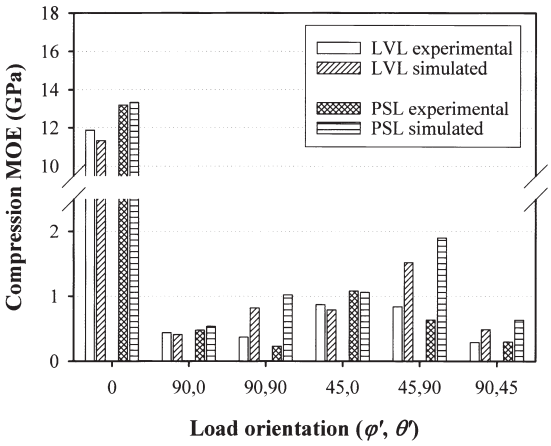

FIG. 6. Experimental and simulated compression MOE of LVL and PSL in the selected six combinations of directions.

sionally oblique, consolidated wood strands or veneers properly over the entire spatial domain.

Figures 7a and b show orthotropic compression diagrams generated from the average simulated and experimental compression MOE of LVL, respectively, using the orthotropic tensor theory (Szalai 1994). Details c and d on this figure depict similar diagrams for PSL. The simulated and actual compression MOE values apparently coincide in the *x-y* plane. However, as the layer or strand orientation (θ') increases over approximately 25º, the trends of the model predictions are reversed compared to trends observed. No such deviations in trends could be observed when the orthotropic models were validated using solid wood specimens (Lang et al. 2002). The veneer manufacturing process may have introduced cracks, compression sets that altered the rolling shear resistance of the veneers; or the densification affected the out-of-plane deformation under compression. This phenomenon needs further investigation.

Nevertheless, these models have practical importance because they can predict the expected elastic response of LVL and PSL with excellent accuracy from the mechanical properties of their constituents in the majority of structural loading conditions. These include support reactions, columns, edgewise beam, and rafter applications where the direction of normal stresses generated by external loads usually coincides with the *x-y* plane of the composites.

Sensitivity analysis was performed to further demonstrate the practicality of the developed simulation models. The analysis consisted of simulating the flatwise-bending MOE of PSL, while progressively reducing the scale parameter (standard deviation) of the distribution of strand angle (α) and strand deviation (β). The examined ranges were between 100% and 0% of the scale parameters, i.e., decreasing the variance of α and β from their original level to no variation at all. Other parameters (e.g., strand thickness, the number of strands and the mean value of α and β) were kept constant.

Figure 8 shows the bending MOE of PSL, as a function of the standard deviation of α and β, expressed by percents of the original standard deviations. As this diagram shows, decreasing the deviation of β from its mean value has little effect on the MOE of PSL. On the other hand, changing the variance of α affects the MOE significantly. Bending MOE improves more than 12% (nearly 2 GPa), if the variation is completely eliminated. This is unfortunately not possible for PSL. However, if by some innovative means, the standard deviation could be reduced by 50%, it would still increase the bending MOE by 8.5%, provided that the other parameters do not change.

The above analysis required minimal modification to the simulation model. Other investigations may involve more significant programming tasks depending on the complexity of the problem to be analyzed.

SUMMARY AND CONCLUSIONS

The bending and orthotropic compression MOE of LVL and PSL have been modeled through simulating the cross-sectional geometry of the composites and the elastic parameters of the constituents. In general, good agreements have been found between simulated and experimental characteristics.

Despite their simplicity, the models reconstructed the geometric structure and density of the composites reasonably well. Analytical

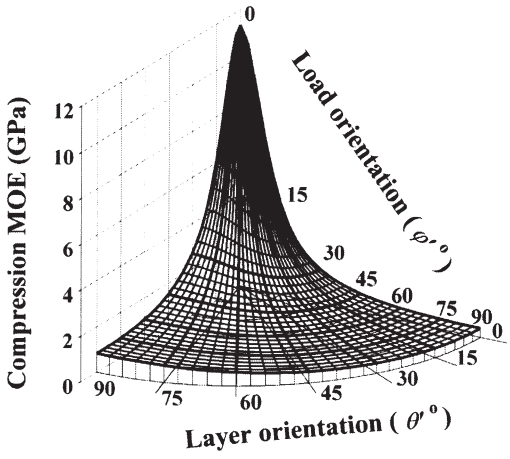

a. – LVL – simulated compression MOE

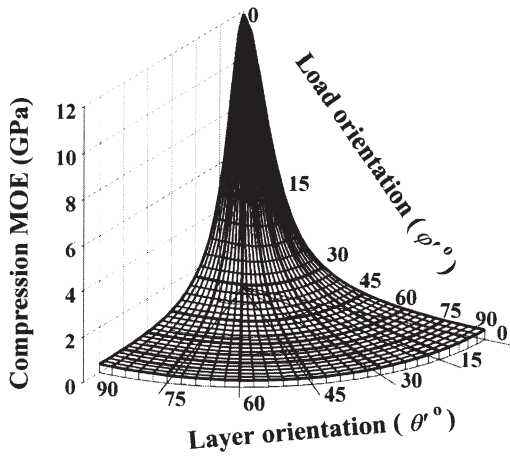

b. – LVL – experimental compression MOE

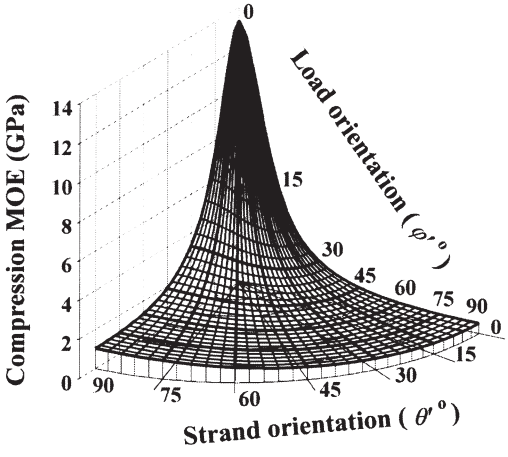

c. – PSL – simulated compression MOE

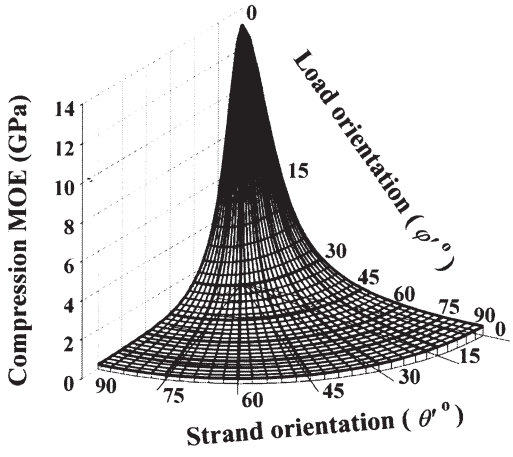

d. – PSL – experimental compression MOE

FIG. 7. Orthotropic diagrams of the simulated and experimental compression MOE of the composites.

works revealed the difficulties in modeling the modulus of elasticity of spatially oblique wood constituents. It has been concluded that the rolling shear in spatially off-axis strands and veneers may significantly influence the apparent modulus of elasticity in compression or in bending. Further research is needed to enhance existing orthotropic models to address the rolling shear deformation and its effect on the elastic response of wood based composites. On the other hand, it has been shown that the elastic performance of the examined composites can be predicted with excellent accuracy if the normal stresses are parallel to the principal *x-y* plane of the structural elements.

Presumably, the practices described under model development, the developed functions, and the module that contains species-specific information provide useful tools for research and development. The discussed work might aid re-

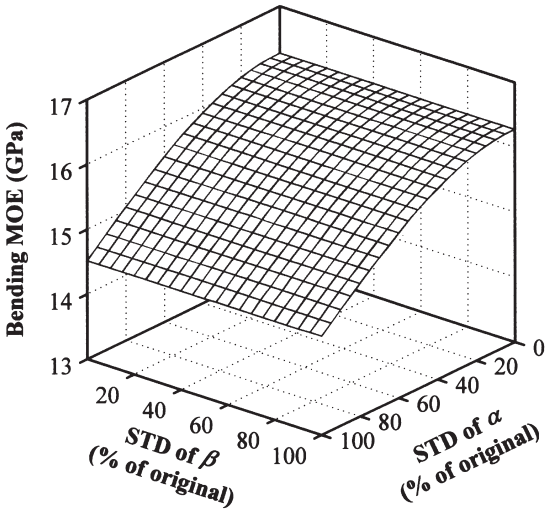

FIG. 8. The effect of decreasing the variation OF α and β on the flatwise, bending MOE of PSL.

search targeted to enlarge the raw material basis or introduce novel design in the structural composite manufacture.

ACKNOWLEDGMENTS

This research was partially financed by the McIntire-Stennis Forestry Research Act, project No. 978 at West Virginia University. The authors wish to express their appreciation to Trus Joist McMillan a Weyerhaeuser Business, LVL and PSL plant at Buckhannon, WV, for donating SCL materials and providing technical assistance in veneer manufacturing. This manuscript is published with the approval of the Director of the West Virginia Agricultural and Forestry Experiment Station as Scientific Article No. 2857.

REFERENCES

AMERICAN SOCIETY FOR TESTING AND MATERIALS (ASTM). 1996a. Standard methods of static tests of lumber in structural size. ASTM D 198–94. ASTM, West Conshohocken, PA.

———. 1996b. Standard test methods for specific gravity of wood and wood-base materials ASTM D 2395–93. ASTM, West Conshohocken, PA.

———. 1996c. Standard test methods for direct moisture content measurement of wood and wood-base materials ASTM D 4442–92. ASTM, West Conshohocken, PA.

———. 1996d. Standard methods of testing small clear specimens of timber. ASTM D 143–94. ASTM, West Conshohocken, PA.

BARNES, D. 2001. A model of the effect of strand length and strand thickness on the strength properties of oriented wood composites. Forest Prod. J. 51(2):36–46.

BODIG, J., AND B. A. JAYNE. 1982. Mechanics of wood and wood composites. Van Nostrand Reinhold Co., New York, NY.

CONNERS, T. E., AND P. J. MEDVECZ. 1992. Wood as a bimodular material. Wood Fiber Sci. 24(4):413–423.

DAI, C., AND P. R. STEINER. 1993. Compression behavior of randomly formed wood flake mats. Wood Fiber Sci. 25(4):349–358.

———, AND ———. 1994a. Spatial structure of wood composites in relation to processing and performance characteristics. Part 2. Modelling and simulation of a randomly-formed flake layer network. Wood Sci. Technol. 28:135–146.

———, AND ———. 1994b. Spatial structure of wood composites in relation to processing and performance characteristics. Part 3. Modelling the formation of multilayered random flake mats. Wood Sci. Technol. 28:229–329.

HALL, P. 1988. Introduction to the theory of coverage processes. John Wiley and Sons, New York, NY.

HARLESS, T. E., F. G. WAGNER, R. D. SEALE, P. H. MITCHELL, AND D. S. LADD. 1987. A model to predict the density profile of particleboard. Wood Fiber Sci. 19(1):81–92.

HARRIS, R. A., AND J. A. JOHNSON. 1982. Characterization of flake orientation in flakeboard by the Von Mises probability distribution function. Wood Fiber 14(4):254–266.

HUMPHREY, P. E., AND A. J. BOLTON. 1989. The hot pressing of dry-formed wood-based composites. Part II. A simulation model for heat and moisture transfer, and typical results. Holzforschung 43:199–206.

KALLMES, O., AND H. CORTE. 1960. The structure of paper. I. The statistical geometry of an ideal two-dimensional fiber network. TAPPI 43(9):737–752.

———, ———, AND G. BERNIER. 1961. The structure of paper. II. The statistical geometry of a multiplanar fiber network. TAPPI 44(7):519–528.

LANG, E. M., AND M. P. WOLCOTT. 1996a. Model for viscoelastic consolidation of wood-strand mats. Part I: Structural characterization of the at via Monte Carlo simulation. Wood Fiber Sci. 28(1) 1996, pp. 100–109.

———, AND ———. 1996b. Model for viscoelastic consolidation of wood-strand mats. Part II: Static stress-strain behavior of the mat. Wood Fiber Sci. 28(3) 1996, pp. 369–379.

———, L. BEJO, J. SZALAI, AND Z. KOVACS. 2000. Orthotropic strength and elasticity of hardwoods in relation to composite manufacture. Part II: Orthotropy of shear strength. Wood Fiber Sci. 32(4):502–519.

———, ———, ———, ———, AND R. B. ANDERSON. 2002. Orthotropic strength and elasticity of hardwoods in relation to composite manufacture. Part II: Orthotropy of

compression strength and elasticity. Wood Fiber Sci. 34(2):350–365.

———, ———, F. Divos, Z. Kovacs, and R. B. Anderson. 2003. Orthotropic strength and elasticity of hardwoods in relation to composite manufacture. Part III: Orthotropic elasticity of structural veneers. Wood Fiber Sci. 35(2):308–320.

Law, A. M., and W. D. Kelton. 1991. Simulation modeling and analysis. 2nd ed. McGraw-Hill, Inc. New York, NY. 759 pp.

Lenth, C. A., and F. A. Kamke. 1996a. Investigations of flakeboard mat consolidation. Part I. Characterizing the cellular structure. Wood Fiber Sci. 28(2):153–167.

———, and ———. 1996b. Investigations of flakeboard mat consolidation. Part II. Modeling mat consolidation using theories of cellular materials. Wood Fiber Sci. 28(3):309–319.

Lu, C., P. R. Steiner, and F. Lam. 1998. Simulation study of wood-flake composite mat structures. Forest Prod. J. 48(5):89–93.

Song, D., and S. Ellis. 1997. Localized properties in flakeboard: A simulation using stacked flakes. Wood Fiber Sci. 29(4):353–363.

Steiner, P. R., and C. Dai. 1993. Spatial structure of wood composites in relation to processing and performance characteristics. Part 1. Rationale for model development. Wood Sci. Technol. 28:45–51.

Suchsland, O. 1967. Behavior of a particleboard mat during the press cycle. Forest Prod. J. 17(2):51–57.

———, and H. Xu. 1989. A simulation of the horizontal density distribution in a flakeboard. Forest Prod. J. 39(5):29–33.

———, and ———. 1991. Model analysis of flakeboard variables. Forest Prod. J. 41(11/12):55–60.

Szalai, J. 1994. Anisotropic strength and elasticity of wood and wood based composites. Private ed. Sopron, Hungary. 398 pp. (in Hungarian.)

Triche, M. H., and M. O. Hunt. 1993. Modeling of parallel-aligned wood strand composites. Forest Prod. J. 43(11/12):33–44.

Wang, K., and F. Lam. 1998. Robot-based research on three-layer oriented flakeboards. Wood Fiber Sci. 30(4):339–347.

Xu, W. 1999. Influence of vertical density distribution on bending modulus of elasticity of wood composite panels: A theoretical consideration. Wood Fiber Sci. 31(3):277–282.

———. 2000. Influence of percent alignment and shelling ratio on modulus of elasticity of oriented strandboard: A model investigation. Forest Prod. J. 50(10):43–47.

Xu, W., and P. R. Steiner. 1995. A statistical characterization of the horizontal density distribution in flakeboard. Wood Fiber Sci. 27(2):160–167.

———, and O. Suchsland. 1997. Linear expansion of wood composites: A model. Wood Fiber Sci. 29(3):272–281.

———, and ———. 1998a. Influence of out-of-plane orientation of particles on linear expansion of particleboard: A simulation study. Forest Prod. J. 48(6):85–87.

———, and ———. 1998b. Modulus of elasticity of wood composite panels with uniform vertical density profile: A model. Wood Fiber Sci. 30(3):293–300.

———, and P. M. Winistorfer. 1996. Fitting an equation to density profile data using Fourier analysis. Holz Roh-Werkst. 54(1):57–59.

Zombori, B. G. 2001. Modeling the transient effects during the hot-pressing of wood-based composites. Ph.D. Dissertation, Virginia Polytechnic Inst. and State University, Blacksburg, VA. 212 pp.